First investigations for a synthetic covariance matrix for monitoring by terrestrial laser scanning

Stephanie Kauker, Volker Schwieger
Institute of Engineering Geodesy,
University of Stuttgart, Germany

Abstract. Modelling correlations within laser scanning point clouds can be achieved by using synthetic covariance matrices. These are based on the elementary error model which contains different groups of correlations: non-correlating, functional correlating and stochastic correlating. By applying the elementary error model on terrestrial laser scanning several groups of error sources should be considered: instrumental, atmospheric and object based. This contribution presents first calculations for the Leica HDS 7000 measuring on small test pieces made of gypsum and aluminum. The determined variances and the spatial correlations of the points are estimated and discussed. Hereby, the mean standard deviation of the point cloud is up to 2.5 *mm* and the mean correlation is about 0.94.

Keywords. Synthetic covariance matrix, elementary error model, terrestrial laser scanning

1 Introduction

Terrestrial laserscanning has become a common tool for deformation and displacement measurements in the geodetic field. In order to guarantee the quality of measurements and to get realistic deformation and analysis results, it is essential to be aware of all error sources and their impact on the measurements. A synthetic covariance matrix for terrestrial laser scanning is necessary in order to model the impacts of the main error sources on the variances and the covariances and correlations respectively within point clouds. These correlations describe stochastic relations among several measurements assuming multi-dimensional normal distributed measurements. The covariance matrix can be modelled by applying the elementary error model (Schwieger, 1999). Based on this model these impacts must be classified into different correlation groups first. Since Schwieger (1999) introduced a third group of correlations, non-correlating, functional correlating and stochastic correlating elementary errors can be differentiated. Each group requires an influencing matrix and a covariance matrix. In Koch (2008a) a similar procedure based on JCGM (1998) and ISO (1995) is developed. The main difference to this contribution is the introduction of non-linear relationships between influencing errors and measured point clouds and the error propagation via Monte Carlo Simulation instead using the law of error propagation. Koch (2008a, 2008b) did not model correlations among the error sources, but show the influence of correlations among the observations on estimated parameters.

In this contribution the influencing matrix contains appropriate impacts of the elementary errors on the point coordinates of the point clouds. For defining the covariance matrix, the variances and, if stochastic correlating errors are considered, the covariances of the elementary errors have to be known. These can be defined by using empirical investigations or manufacturers' information, among others. Next, the elementary error model has to be applied on all the error sources which affect observations. These include instrumental, atmospheric and object based errors. The instrumental error group comprises, e.g. zero point error, collimation axis error, vertical collimation error and tumbling error. Furthermore, the atmospheric group consists of air temperature, air pressure and partial water vapour pressure. Regarding objects, the impact of errors, such as angle of incidence and reflectivity, should be taken into account. Afterwards, the synthetic covariance matrix can be computed. The results show that the impact of instrumental and atmospheric errors may cause standard deviations of a few mm.

The investigations are executed within the project "Integrated spatio-temporal modelling using correlated observations for the derivation of surveying configurations and description of deformation processes" (IMKAD).

2 Elementary error model and synthetic covariance matrix

In this section, the structure of the elementary error model and its link to the synthetic covariance matrix are described.

2.1 Elementary errors

Since Hagen (1837) and Bessel (1837) established the elementary error model, observations, such as horizontal and vertical angle and distances, can be treated as random quantities. That implies that any realisation l of a measured random quantity L deviates from its expected value μ_l by random deviation ε (Schwieger, 1999). This is, any random deviation may be presented by a sum of numerous, very small elementary errors d_i:

$$\mu_l = l - \varepsilon, \qquad and \quad \varepsilon = \sum_{i=1}^{v} d_i \,. \tag{1}$$

Assuming that each elementary error contains the same absolute value, negative and positive sign may be equally probable (Hagen, 1837). Consequently, according to the central limit theorem Pelzer (1985) determines the expected value of the random deviation μ_ε to zero:

$$\mu_\varepsilon = E(\varepsilon) = \sum_{i=1}^{v} E(d_i) = 0. \tag{2}$$

The authors assume that systematic effects do not occur or, more precisely, are randomized. On closer inspection, however, it is revealed that the number of elementary errors increases in case of a decrease regarding their absolute values. Hence, on the assumption of infinite elementary errors, their absolute values may be infinitely small. For this reason, assuming standard normal distribution is justified for standardized random deviations ε. In consequence, normal distribution is applicable to the measured random quantity L, considering standard deviation σ and variance σ^2 (Pelzer, 1985):

$$\bar{\varepsilon} = \frac{\varepsilon}{\sigma} \sim N(0,1), \qquad and \quad L \sim N(\mu_l, \sigma^2). \tag{3}$$

In general, modelling normal distributed measurements is based on a sum of very small elementary errors with changing signs. Due to multidimensional observations and their related random deviations, the scalars shown in eq. (1) and eq. (2) are n-dimensional vectors (Pelzer, 1985):

$$\boldsymbol{\mu_l} = \boldsymbol{l} - \boldsymbol{\varepsilon}, \qquad and \quad \boldsymbol{E(\varepsilon)} = \sum_{i=1}^{v} \boldsymbol{E(d)} = \boldsymbol{0}. \tag{4}$$

Besides, handling multi-dimensional data requires the classification of elementary errors. In order to model the impact on the observations influence factors are used for building influencing matrices.

These matrices contain the effect on the covariance matrix of the observations. Schwieger (1999) considers three types of correlations which are classified below:

- p non-correlating error vectors $\boldsymbol{\delta_k}$,
- m functional correlating errors ξ_j ,
- q stochastic correlating error vectors $\boldsymbol{\gamma_h}$,

$$\boldsymbol{\delta_k} = \begin{bmatrix} \delta_{1k} \\ \delta_{2k} \\ \vdots \\ \delta_{nk} \end{bmatrix}, k = 1,2,\dots,p, \qquad \boldsymbol{\xi} = \begin{bmatrix} \xi_1 \\ \xi_2 \\ \vdots \\ \xi_m \end{bmatrix}, \quad and \quad \boldsymbol{\gamma_h} = \begin{bmatrix} \gamma_{1h} \\ \gamma_{2h} \\ \vdots \\ \gamma_{nh} \end{bmatrix}, h = 1,2,\dots,q \,, \tag{5}$$

where the index n defines the number of observations. Regarding the non-correlating errors, k specifies the kind of elementary errors, whereas p describes the number of elementary errors. The index m represents the number of functional correlating elementary errors ξ_j. Additionally, the index h involves the type of stochastically classified elementary errors and q implies the number of stochastic correlating errors.

The next step is to model the impact on the measurements. This can be implemented by partial derivatives, which have to be determined analytically or numerically. Schwieger (1999) induces the influences of different elementary errors on the observations by integrating the derivatives into influencing matrices.

As mentioned above, three types of errors have to be considered which can now be computed as follows:

- p matrices $\boldsymbol{D_k}$ for non-correlating errors,
- one matrix $\boldsymbol{F}$ for functional correlating errors,
- q matrices $\boldsymbol{G_h}$ for stochastic correlating errors.

Based on the model assumption the influencing matrices characterise the projection of the elementary errors into the observation space.

The structures of the influencing matrices are different from each other because several elementary errors affect the measurements differently. The matrices $\boldsymbol{D_k}$ and $\boldsymbol{G_h}$ are diagonally structured because each elementary error of the non-correlating and stochastic correlating classes influences exactly one measurement quantity functionally (see eq. (6)). In contrast to these cases, matrix $\boldsymbol{F}$ is not structured diagonally, since one functional correlating error may impact more than one measurement quantity (Schwieger, 1999). To

clarify this, the elements of $\boldsymbol{D_k}$, $\boldsymbol{F}$ and $\boldsymbol{G_h}$ are shown below:

$$\boldsymbol{D_k} = \begin{bmatrix} \frac{\partial l_1}{\partial \delta_{1k}} & 0 & \cdots & 0 \\ 0 & \frac{\partial l_2}{\partial \delta_{2k}} & 0 & \vdots \\ \vdots & 0 & \ddots & \vdots \\ 0 & \cdots & \cdots & \frac{\partial l_n}{\partial \delta_{nk}} \end{bmatrix}, \boldsymbol{F} = \begin{bmatrix} \frac{\partial l_1}{\partial \xi_1} & \frac{\partial l_1}{\partial \xi_2} & \cdots & \frac{\partial l_1}{\partial \xi_m} \\ \frac{\partial l_2}{\partial \xi_1} & \frac{\partial l_2}{\partial \xi_2} & \cdots & \frac{\partial l_2}{\partial \xi_m} \\ \vdots & \vdots & \ddots & \vdots \\ \frac{\partial l_n}{\partial \xi_1} & \frac{\partial l_n}{\partial \xi_2} & \cdots & \frac{\partial l_n}{\partial \xi_m} \end{bmatrix}, \quad (6)$$

$$\boldsymbol{G_h} = \begin{bmatrix} \frac{\partial l_1}{\partial \gamma_{1h}} & 0 & \cdots & 0 \\ 0 & \frac{\partial l_2}{\partial \gamma_{2h}} & 0 & \vdots \\ \vdots & 0 & \ddots & \vdots \\ 0 & \cdots & \cdots & \frac{\partial l_n}{\partial \gamma_{nh}} \end{bmatrix}.$$

Summing up all elementary errors results in the random deviation vector $\boldsymbol{\varepsilon}$. Consequently, Schwieger (1999) considers the projection into the observation space as:

$$\boldsymbol{\varepsilon} = \sum_{k=1}^{p} \boldsymbol{D_k} \cdot \boldsymbol{\delta_k} + \boldsymbol{F} \cdot \boldsymbol{\xi} + \sum_{h=1}^{q} \boldsymbol{G_h} \cdot \boldsymbol{\gamma_h} \ . \quad (7)$$

2.2 Synthetic covariance matrix

For the construction of a synthetic covariance matrix the elementary error model is essential. The determination of variances, covariances and correlations for observations is realised by means of a covariance matrix $\boldsymbol{\Sigma_{ll}}$ which is generally structured as shown below:

$$\boldsymbol{\Sigma_{ll}} = \begin{bmatrix} \sigma_1^2 & \sigma_{12} & \cdots & \sigma_{1n} \\ \sigma_{12} & \sigma_2^2 & \cdots & \sigma_{2n} \\ \vdots & \vdots & \ddots & \vdots \\ \sigma_{1n} & \sigma_{2n} & \cdots & \sigma_n^2 \end{bmatrix}. \quad (8)$$

The elements on the main diagonal, $\sigma_1^2 \ldots \sigma_n^2$, remain the variances which present the stochastic dependence of one random value, with index n defining the number of measurements. The σ-values located on the secondary diagonals contain the covariance between two observations. By means of the covariance and the square root of the variances, the correlation coefficient ρ can be determined (Benning, 2010):

$$\rho = \frac{\sigma_{12}}{\sigma_1 \cdot \sigma_2} \ . \quad (9)$$

Summing up each covariance matrix of the several types of elementary errors results in the so called "*synthetic covariance matrix*" $\boldsymbol{\Sigma_{ll}}$. Applying the law of error propagation on eq. (7) the equation of the synthetic covariance matrix is determined (Schwieger, 1999):

$$\boldsymbol{\Sigma_{ll}} = \sum_{k=1}^{p} \boldsymbol{D_k} \cdot \boldsymbol{\Sigma_{\delta\delta,k}} \cdot \boldsymbol{D_k^T} + \boldsymbol{F} \cdot \boldsymbol{\Sigma_{\xi\xi}} \cdot \boldsymbol{F^T} + \sum_{h=1}^{q} \boldsymbol{G_h} \cdot \boldsymbol{\Sigma_{\gamma\gamma,h}} \cdot \boldsymbol{G_h^T} \ . \quad (10)$$

In the following the covariance matrices of the elementary errors are defined:

- $\boldsymbol{\Sigma_{\delta\delta,k}}$ the covariance matrix for the non-correlating errors,
- $\boldsymbol{\Sigma_{\xi\xi}}$ the covariance matrix for the functional correlating errors,
- $\boldsymbol{\Sigma_{\gamma\gamma,h}}$ the covariance matrix for the stochastic correlating errors.

In this context, the matrices $\boldsymbol{\Sigma_{\delta\delta,k}}$ and $\boldsymbol{\Sigma_{\xi\xi}}$ are structured diagonally and only filled on the main diagonal (see eq. (11)). As a result, modelling correlations among the elementary errors is avoided, e.g., in case k=1, multiplying $\boldsymbol{D_1}$ and $\boldsymbol{\Sigma_{\delta\delta,1}}$ leads to a new matrix which is filled only on the main diagonal.

$$\boldsymbol{\Sigma_{\delta\delta,k}} = \begin{bmatrix} \sigma_{1k}^2 & 0 & \cdots & 0 \\ 0 & \sigma_{2k}^2 & 0 & \vdots \\ \vdots & 0 & \ddots & \vdots \\ 0 & \cdots & \cdots & \sigma_{nk}^2 \end{bmatrix}$$

$$\boldsymbol{\Sigma_{\xi\xi}} = \begin{bmatrix} \sigma_1^2 & 0 & \cdots & 0 \\ 0 & \sigma_2^2 & \cdots & \vdots \\ \vdots & \vdots & \ddots & \vdots \\ 0 & \cdots & \cdots & \sigma_m^2 \end{bmatrix}, \quad (11)$$

$$\boldsymbol{\Sigma_{\gamma\gamma,h}} = \begin{bmatrix} \sigma_{1h}^2 & \sigma_{12h} & \cdots & \sigma_{1nh} \\ \sigma_{12h} & \sigma_{2h}^2 & \cdots & \sigma_{2nh} \\ \vdots & \vdots & \ddots & \vdots \\ \sigma_{1nh} & \cdots & \cdots & \sigma_{nh}^2 \end{bmatrix}.$$

The covariance matrix $\boldsymbol{\Sigma_{\gamma\gamma,h}}$ comprises covariances among the elementary errors of one type and can be completely filled. Its structure is not diagonal. Moreover, the related influencing matrix $\boldsymbol{G_h}$ consists of functional independent values.

In the next step, variances and covariances, in case of stochastic correlating errors, for all groups of errors have to be determined. This turns out to be a challenging part because correlations between the elementary errors are not known. Thus, they may be specified by using manufacturers' information, empirical values or by an estimation based on maximum errors. According to Pelzer (1985) one can estimate the standard deviation of an elementary error by means of its maximum error (see eq. (20)). For this, the probability distribution must be known. In case of a rectangular distribution the maximum error must be multiplied by 0.6, in case of a triangular distribution the factor 0.4 is applied and for normal distribution one use 0.3. Regarding the stochastic correlating group, realistic values for estimating the stochastical correlations must be known. These represent stochastic relations for multi-dimensional normal distributed observations.

3 Application of the Elementary Error Model on Terrestrial Laser Scanner

In order to apply the elementary error model on terrestrial laser scanners, all fundamental sources of errors must be identified first. On the one hand, measurements are affected by the manufacturing accuracy of the instrument itself. On the other hand, the laser beam is affected by the atmosphere while it runs through. And finally, the monitored object influences the observations due to its surface characteristics and colour (Kauker and Schwieger, 2015). Errors that may be not covered by this analysis are modelled stochastically and are covered by the noise matrix, see equation (13).

3.1 Elementary errors of a terrestrial laser scanner

There are different systems of terrestrial laser scanners (TLS) such as panorama scanners, hybrid scanners and camera scanners. However, in this paper a panorama scanner is used, the Leica HDS 7000. For this reason the description of the construction is limited to this kind of type. The remaining types of scanners are detailed in, e.g., Eling (2009).

A panorama scanner consists of a rotating sloped mirror (see Fig. 1) and offers a full panorama with a field of view of 360° horizontally and 320° vertically. The slope distance s, the horizontal angle λ and the vertical angle ϑ define the polar observables. In order to determine the scanned points in the observation space, these elements have to be known. Next, Cartesian coordinates can be calculated for each point.

Figure 1 shows the geometrical relation between the polar observables $s,\ \lambda,\ \vartheta$ and the Cartesian Coordinates $X,\ Y,\ Z$. The transformation can be calculated as follows:

$$\begin{bmatrix} X \\ Y \\ Z \end{bmatrix} = s \begin{bmatrix} \sin\vartheta \cos\lambda \\ \sin\vartheta \sin\lambda \\ \cos\vartheta \end{bmatrix} \tag{12}$$

Due to previous investigations, e.g. Deumlich and Staiger (2002), Lichti and Lampard (2008) and Lichti (2010), it is assumed that the main function of a terrestrial laser scanner is similar to a total station. Accordingly, it can be assumed that the main error sources of a total station may also appear for a terrestrial laser scanner. Moreover, their three axes like collimation axis, horizontal axis and vertical axis are comparable. In consequence, their errors can be applied. Deviating from that, Holst

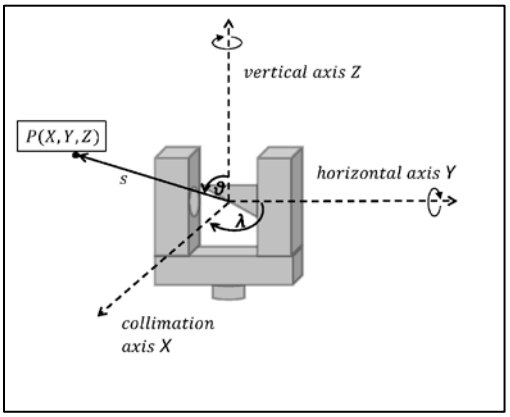

Fig 1: Main construction elements of a TLS

and Kuhlmann (2011) and Holst et al. (2014) use a different approach.

First, the elementary errors are classified into instrumental, atmospheric and object based errors. Next, the errors sources are grouped regarding the three types of correlations mentioned in section 2. In this project, the following instrumental errors are investigated: range noise and angular noise, scale error, zero point error, collimation axis error, horizontal axis error, vertical index error, tumbling error and eccentricity of the collimation axis. Most of the instrumental errors belong to the functional correlated group. Only range noise and angular noise are classified to the non-correlated elementary errors.

The data sheet of the HDS 7000 (Leica Geosystems, 2011) provides the standard deviations of these two errors: the range noise σ_r is 0.5 mm and angular noise σ_a is 125 μrad.

The influencing matrix $\boldsymbol{D}$ is equivalent to the identity matrix $\boldsymbol{I}$. Regarding one measurement, this leads to:

$$\boldsymbol{\Sigma}_{\delta\delta,1} = \begin{bmatrix} \sigma_a^2 & 0 & 0 \\ 0 & \sigma_a^2 & 0 \\ 0 & 0 & \sigma_r^2 \end{bmatrix}, \qquad \boldsymbol{D} = \boldsymbol{I}\ . \tag{13}$$

According to Stahlberg (1997), Neitzel (2006a) and Neitzel (2006b) the functional relations among the further instrumental error sources can be computed as follows:

$$s_k = k_0 + s \cdot m_0 \tag{14}$$

$$\theta_k = acos(\cos i_0 \cdot \cos c_0 \cdot \cos(\zeta + \Delta\zeta + h_0) - \sin i_0 \cdot \sin c_0) \tag{15}$$

$$\lambda_k = \alpha + \Delta\alpha + \frac{e_z}{s_k \cdot \sin(\zeta + \Delta\zeta + h_0)} + atan\left(\frac{\cos i_0 \cdot \tan c_0}{\sin(\zeta + \Delta\zeta + h_0)} + \frac{\sin i_0}{\tan(\zeta + \Delta\zeta + h_0)}\right). \tag{16}$$

Here the index k defines the corrected observables. The further parameters are defined as follows:

s:	measured slope distance
k_0:	zero point error
m_0:	scale error
c_0:	collimation axis error
i_0:	horizontal axis error
h_0:	vertical index error
v_0:	tumbling error
e_z:	eccentricity of the collimation axis
α:	measured horizontal rotation angle
ζ:	measured vertical rotation angle
s_k:	corrected slope distance
λ_k:	corrected horizontal rotation angle (horizontal angle)
θ_k:	corrected vertical rotation angle (zenith angle)

While rotating around the vertical axis a tumbling error may occur. This additionally affects the observed values. This error is investigated by Neitzel (2006b). The impact of this error can be approximated by the functional model as follows, whereby α_z represents the horizontal direction of the projection of the zenith angle into the horizontal plane. ζ_z defines the angle between the vertical axis and the direction to the zenith:

$$\Delta\alpha = v_0 \cdot \sin\alpha_z \cdot \cot\zeta_z \quad (17)$$

$$\Delta\zeta = v_0 \cdot \cos\alpha_z \quad (18)$$

In order to fill the related influencing matrix $\boldsymbol{F}$, the partial derivatives of eq. (14) to eq. (18) are necessary. Moreover, it is substantial to define variances for constructing the covariance matrix $\boldsymbol{\Sigma_{\xi\xi}}$. Its structure is shown below:

$$\boldsymbol{\Sigma_{\xi\xi}} = \begin{bmatrix} \sigma_{m_0}^2 & 0 & \cdots & & & \cdots & 0 \\ 0 & \sigma_{k_0}^2 & & & & & \vdots \\ \vdots & & \sigma_{c_0}^2 & & & & \\ & & & \sigma_{i_0}^2 & & & \\ & & & & \sigma_{h_0}^2 & & \vdots \\ \vdots & & & & & \sigma_{v_0}^2 & 0 \\ 0 & \cdots & & & \cdots & 0 & \sigma_{e_z}^2 \end{bmatrix}. \quad (19)$$

In Gordon (2008) some of these values are investigated, where the zero point error shows a maximum value up to 5 *mm*, the maximum value of the vertical index error is -17.69 *mgon* and the maximum value of the collimation axis error is -19.62 *mgon*. According to Neitzel (2006a), the maximum value of the horizontal axis error is up to -14.6 *mgon* among others. Thus, these values can be used for the approach. Furthermore, the scale error and the eccentricity of the collimation axis are investigated by Gordon (2008).

In case the standard deviation σ_k as well as the respective probability distribution of an error δ_{ik} is not known, the best and most probable assumption is the normal distribution (Pelzer, 1985):

$$\sigma_k \approx 0.3 \cdot \delta_{ik}[max] \quad (20)$$

All standard deviations of the instrumental errors used for creating the corresponding covariance matrices are shown in table 1 below.

Table 1: Standard deviations of instrumental errors

Error source	Standard deviation
range noise	0.5 [*mm*]
angle noise	125 [μrad]
scale error	0.300018 [*mm/km*]
zero point error	1.50 [*mm*]
collimation axis error	5.89 [*mgon*]
horizontal axis error	4.38 [*mgon*]
vertical index error	5.31 [*mgon*]
tumbling error	0.06 [*mm/m*]
eccentricity of the collimation axis	0.60 [*mm*]

3.2 Elementary errors of the atmosphere

As mentioned above the laser beam is also affected by the atmosphere while running through. Computing its impact on the observed values requires modelling of the environmental influences, such as air temperature, air pressure and partial water vapour pressure. The speed of propagation of electromagnetic waves depends on the refractive index *n*, the density of the atmospheric layer and the wavelength itself. According to Ciddor (1996) and Ciddor and Hill (1999), the group refractive index n_{Gr} for a dry standard atmosphere, that is drying temperature t = 0 *°C*, pressure p = 1013.25 *hPa*, partial water vapour pressure e = 0 *hPa*, CO_2-content = 0.0375 % = 375 *ppm*, can be determined as follows:

$$N_{Gr} = (n_{Gr} - 1) \cdot 10^6 = 287.6155 + \frac{4.88660}{\lambda^2} + \frac{0.06800}{\lambda^4} \quad (21)$$

with N_{Gr} presenting the group refractive index of light for normal atmosphere and λ defining the wavelength. As shown in eq. (21), the refractive index is dependent on the wavelength. In order to calculate the impact, the standard atmosphere must be reduced to real atmospheric conditions (Joeckel et al., 2008):

$$N_L = (n_L - 1) \cdot 10^6 = N_{Gr} \cdot \frac{273.15}{1013.25}\frac{p}{T} - \frac{11.27}{T \cdot e} \quad (22)$$

with N_L comprising the reduction of the standard atmosphere to the current atmospheric environment, n_L defining the group refractive index of light with current environment and T describing the temperature ($T = t + 273.15$ *K*). Hereby, the scope of eq. (22) is limited to t ranging between – 40 *°C*, …, +100 *°C*, p ranging between 800-1200 *hPa* and

0… 100% relative humidity. The accuracy is at 0.5 *ppm*.
Based on eq. (22) the total differential can be calculated:

$$\partial N_L = \frac{\partial n_L}{\partial t} \cdot dt + \frac{\partial n_L}{\partial p} \cdot dp + \frac{\partial n_L}{\partial e} \cdot de \ . \qquad (23)$$

For a mean atmosphere, with temperature of 17 °*C* (T = 290.15 *K*), pressure of 1000 *hPa* and partial water vapour pressure of 11 *hPa*, the differential quotients result in (Joeckel et al., 2008):

$$\begin{aligned} \frac{\partial n_L}{\partial t} &= -1.00 \cdot 10^{-6} \left[\frac{1}{K}\right], \\ \frac{\partial n_L}{\partial p} &= 0.29 \cdot 10^{-6} \left[\frac{1}{hPa}\right], \\ \frac{\partial n_L}{\partial e} &= -0.04 \cdot 10^{-6} \left[\frac{1}{hPa}\right] \end{aligned} \qquad (24)$$

By means of eq. (24), the impact of the atmospheric parameters on distance measurements can be approximated (e.g., Rüeger 1990):

$$\Delta n \cdot 10^6 = -1.00\, \Delta t + 0.29\, \Delta p - 0.04\, \Delta e \qquad (25)$$

Table 2 below shows the impact on the distance measurements depending on changes of temperature, pressure and partial water vapour pressure.

Table 2: Standard deviations of atmospheric errors

	dt / dp / de	**ds**	**g_t / g_p / g_e**
temperature	1 *°C*	1 [*ppm*]	1.00 [*ppm / °C*]
pressure	3.4 *hPa*	1 [*ppm*]	0.29 [*ppm/hPa*]
partial water vapour pressure	25 *hPa*	1 [*ppm*]	0.04 [*ppm/hPa*]

Each of the atmospheric elementary errors is classified to the stochastic correlating group. In order to gain an impression about the impact of the stochastic influencing values, the parameters of table 2 are used. In the next step, it is essential to define variances and covariances for designing the corresponding covariance matrix $\boldsymbol{\Sigma_{\gamma\gamma,h}}$. Regarding one measurement, this leads to:

$$\boldsymbol{\Sigma_{\gamma\gamma,1}} = \begin{bmatrix} \sigma_t^2 & \sigma_{tp} & \sigma_{te} \\ \sigma_{tp} & \sigma_p^2 & \sigma_{pe} \\ \sigma_{te} & \sigma_{pe} & \sigma_e^2 \end{bmatrix}. \qquad (26)$$

In this research it is assumed that these values do not dependent on their location. In this special case the relation is no longer stochastic, but functional. Inevitably, the correlations become ± 1 and the stochastic correlation modelling is changed to functional modelling instead.

3.3 Elementary errors based on the monitored objects

The third source of errors that has to be considered is linked to the surface quality and colour of the monitored objects. After the laser beam hits the object's surface it is immediately reflected. Thereby, the intensity of the reflection depends on the following characteristics of the object.

- Penetration depth
- Roughness
- Reflectivity
- Colour
- Edges

Additionally, the scanning geometry is decisive due to the angle of incidence.

Considering the intensity of a reflected signal at its maximum, there are four attributes affecting the measurements: penetration depth, roughness, reflectivity and colour. Previous investigations, e.g. (Schäfer, 2011) and (Zámečniková and Neuner, 2014), have shown complex connections of phase-based measurements among these four attributes. Based on this knowledge, these four elementary errors are classified as stochastic correlating because a separation is not possible right now. Whereas the angle of incidence and the interaction regarding laser beams hitting edges can be approximated functionally. The bigger the angle of incidence, the less energy of the signal is thrown back. By means of Lambert's cosine law the intensity of the reflected signal is proportional depending on the cosine of the angle of the incident beam.

3.4 Overview of classification

Table 3 below shows the classification of all elementary errors which are investigated in this publication. The elementary errors used for computing $\boldsymbol{\Sigma_{ll}}$ are marked with *.

Table 3: Classification of elementary errors

Type of correlation	Error source	
non	range noise	*
	angle noise	*
stochastic	temperature	*
	pressure	*
	partial water vapour pressure	*
	penetration depth	
	roughness	
	reflectivity	
	colour	
functional	angle of incidence	
	edges	
	scale error	*
	zero point error	*
	collimation axis error	*
	horizontal axis error	*
	vertical index error	*
	tumbling error	*
	eccentricity of the collimation axis	*

4 Simulation

In order to evaluate and improve the model for the synthetic covariance matrix, small sample pieces are necessary. Considering the impact on the laser beam caused by the material, the investigated sample pieces consist of aluminium and gypsum.

4.1 Test pieces

Figure 2 shows two boards of different materials: aluminium and gypsum made by a 3D printer. To compare the impact of these two materials on the observations, both boards are produced with the same size: 30 *cm* x 25 *cm*. After the production both are measured with the API Radian Laser tracker in order to receive reference values for the future evaluation of the synthetic covariance matrix. For computing the synthetic covariance matrix regarding the boards of figure 2, an equivalent angle grid must be generated first. Therefore, the point distance of general scanning settings is chosen: 6.283 *mm* at 5 *m* scanning distance.

In figure 3, the corresponding grid is displayed.

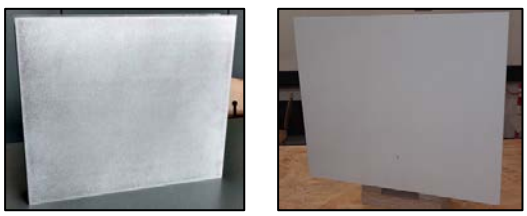

Fig 2: Test pieces (left: aluminium, right: gypsum)

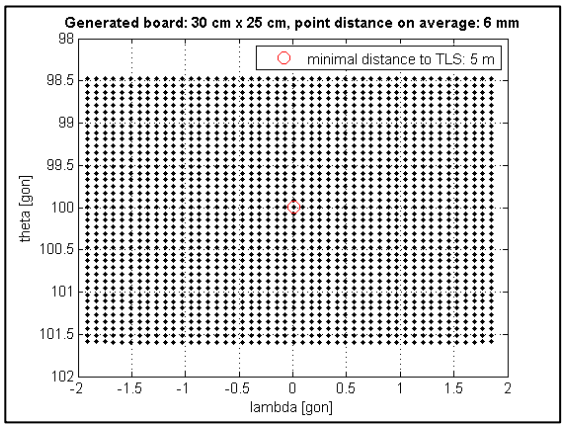

Fig 3: Simulated point cloud, shortest distance in the centre

Next, the synthetic covariance matrix can be computed by using instrumental errors as mentioned in section 3.1. Additionally, the atmospheric conditions within the scanning area have to be considered. Due to the small scanning area it is assumed that the variances and covariances are not dependent on their location. The errors are modelled as functional correlating. For this reason, the same atmospheric values are generated for the whole board using σ_t = 0.01 °*C*, $\sigma_p = \sigma_e = 10^{-8}$ *hPa*. Object based impacts are ignored for the moment.

4.2 Results

According to eq. (10), the synthetic covariance matrix $\boldsymbol{\Sigma_{ll}}$ comprises variances and covariances of all points within the cloud. Due to its structure, given in eq. (27), variances regarding each coordinate axis are available.

$$\boldsymbol{\Sigma_{ll}} = \begin{bmatrix} \sigma_{x_1}^2 & \sigma_{x_1y_1} & \sigma_{x_1z_1} & \cdots & \sigma_{x_1z_n} \\ \sigma_{x_1y_1} & \sigma_{y_1}^2 & \sigma_{y_1z_1} & & \\ \sigma_{x_1y_1} & \sigma_{y_1z_1} & \sigma_{z_1}^2 & & \vdots \\ \vdots & & & \ddots & \\ \sigma_{x_1z_n} & & \cdots & & \sigma_{z_n}^2 \end{bmatrix}. \qquad (27)$$

Afterwards, the error of position (according to Helmert) can be calculated for each point among the cloud by using the variances on the main diagonal (Pelzer, 1985):

$$\sigma_{xyz_i} = \sqrt{\sigma_{x_i}^2 + \sigma_{y_i}^2 + \sigma_{z_i}^2}, \qquad i = 1, \dots, n. \qquad (28)$$

The results are displayed in figure 4. As expected, the positional standard deviation is best in the middle of the board and gets worse in the direction of each corner. Moreover, it is clearly visible that the range between the minimum and the maximum is at 1 μm. This small difference is caused by the

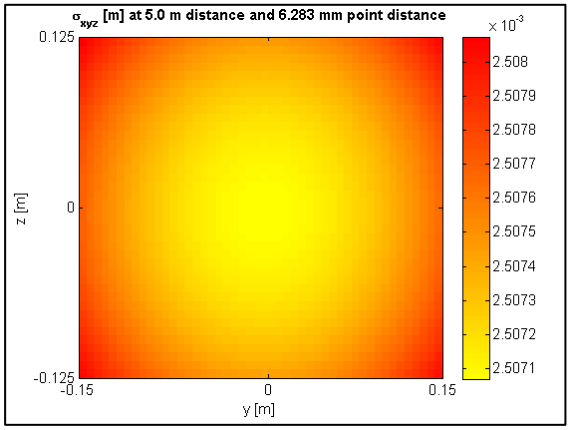

Fig 4: Error of position, minimum at 2.507 mm

small area of the test piece and the ignorance of object based impacts. Nevertheless, these values are particularly pessimistic because some empirical determinations show more optimistic values. The future will show if these values may be evaluated by new empirical ones for the HDS 7000.

In order to determine the correlation matrix $\boldsymbol{R_{ll}}$ which contains the spatial correlations within the point cloud, the synthetic covariance matrix must be standardized as follows:

$$\boldsymbol{R_{ll}} = \frac{1}{\sqrt{diag(\boldsymbol{\Sigma_{ll}})}} * \boldsymbol{\Sigma_{ll}} * \frac{1}{\sqrt{diag(\boldsymbol{\Sigma_{ll}})}} \,. \qquad (29)$$

Due to its structure, that is equal to the one of $\boldsymbol{\Sigma_{ll}}$, correlations for each axis can be calculated easily.

A closer look into the correlations of the x-coordinates confirms the assumption that the correlations depend on the distances to each other. The greater the distance between the coordinates, the less become their spatio correlations. Figure 5 shows a tiny tendency. The differences might be bigger in case the point density is less. This depends on the size of the object, the scanning solution and the distance between TLS and object.

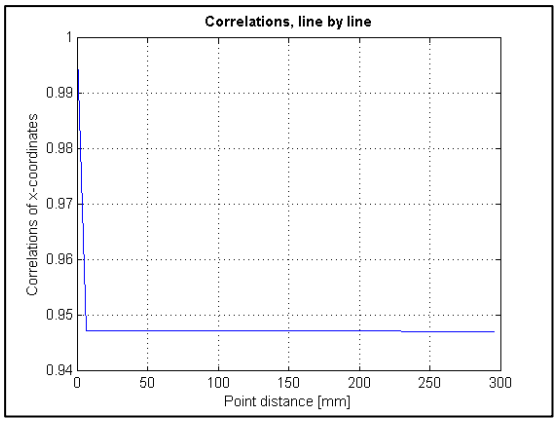

Fig 5: Correlations of x-coordinates depending on their distances to each other

The small variations of the variance as well as the high non-changing correlations are caused by the almost identical influences of the instrumental and atmospheric errors. The object based errors would cause higher variations.

5 Conclusion and future work

Summing up, a model for computing the synthetic covariance matrix for monitoring by terrestrial laser scanning is presented. Hereby, different error sources like instrumental and atmospheric errors are considered. For first calculations the atmospheric impact is simplified due to laboratory scanning conditions. It can be shown that the modelled standard deviations of the point cloud are about 2.5 *mm* which primarily depends on the value of the instrumental error variances and the resolution of the scanning. Furthermore, the correlations of the x-coordinates are investigated. Hereby, it can be noticed that the intensity of the correlations reaches more than 0.95 and is depending on the point distances to each other.

In the next step in the future, the synthetic covariance matrix must be evaluated by empirical values and by multiple scans in order to provide temporal correlations between observations. Moreover, using more realistic instrumental error variances of the HDS 7000 might improve the modelled standard deviations. In addition, it is essential to take object based impacts into account in order to compute the errors as realistically as possible. Furthermore, other test bodies like barrages and dams will be investigated to model atmospheric impacts.

Acknowledgement

The investigations published in this article are granted by the DFG (German Research Foundation) under the sign SCHW 838/7-1. The authors cordially thank the funding agency.

References

Benning, W. (2010): Statistik in Geodäsie, Geoinformation und Bauwesen. 3. Auflage, Wichmann Verlag, Heidelberg, 2010.

Bessel, F. W. (1837): Untersuchungen über die Wahrscheinlichkeit der Beobachtungsfehler. Astronomische Nachrichten, Vol. 15, pages 369-404.

Ciddor, P. E. (1996): Refractive index of air: new equations for the visible and near infrared. Applied Optics, Vol. 35, No. 9, 1566 – 1573.

Ciddor, P. E.; Hill, R. J. (1999): Refractive index of air: 2. Group index. Applied optics, Vol. 38, No. 9, 1663-1667

Deumlich, F.; Staiger, R. (2002): Instrumentenkunde der Vermessungstechnik. 9. Auflage, Herbert Wichmann Verlag, Heidelberg.

Eling, D. (2009): Terrestrisches Laserscanning für die Bauwerksüberwachung. DGK – Deutsche Geodätische Kommission, Reihe C, Nr. 641, Verlag der Bayerischen Akademie der Wissenschaften, München.

Gordon, B. (2008): Zur Bestimmung von Messunsicherheiten terrestrischer Laserscanner. TU Darmstadt, Dissertation, http://tuprints.ulb.tu-darmstadt.de/1206/, last accessed on September, 8 2015.

Hagen, G. (1837): Grundzüge der Wahrscheinlichkeits-Rechnung. Berlin.

Holst, Ch.; Tegelbeckers, J.; Kuhlmann, H. (2014): Erkennung und Erklärung von systematischen Effekten beim TLS, In: Schriftenreihe DVW, Band 78, „Terrestrisches Laserscanning 2014 (TLS 2014)“, Wißner Verlag, S. 51-68

Holst, Ch.; Kuhlmann, H. (2011): Bestimmung der elevationsabhängigen Deformation des Hauptreflektors des 100m-Radioteleskops Effelsberg mit Hilfe von Laserscannermessungen, In: Schriftenreihe DVW, Band 66 „Terrestrisches Laserscanning - TLS 2011 mit TLS-Challenge“, S. 161-180, Wißner Verlag

ISO (1995): Guide to the Expression of Uncertainty in Measurement (GUM), First edition, 1993, corrected and reprinted 1995, International Organisation for Standardization (ISO), Geneva,

JCGM (1998): Evaluation of Measurement Data – Supplement 1 to the “Guide to the Expression of Uncertainty in Measurement” – Propagation of distributions using a Monte Carlo method. JCGM 101:2008. Joint Committee for Guides in Metrology,

Joeckel, R.; Stober, M.; Huep, W. (2008): Elektronische Entfernungsmessung und ihre Integration in aktuelle Positionierungsverfahren. 5. Auflage, Herbert Wichmann Verlag.

Kauker, S.; Schwieger, V. (2015): Approach for a Synthetic Covariance Matrix for Terrestrial Laser Scanner. Proceedings on 2nd International workshop on “Integration of Point- and Area-wise Geodetic Monitoring for Structures and Natural Objects”, March 23-24, 2015, Stuttgart, Germany.

Koch, K. R. (2008a): Evaluation of uncertainties in measurements by Monte Carlo simulations with an application for laserscanning, Journal. Applied Geodesy 2, pages 67-77.

Koch, K. R. (2008b): Determining uncertainties of correlated measurements by Monte Carlo simulations applied to laserscanning, Journal Applied Geodesy 2, 139-147.

Leica Geosystems (2011): Datasheet of HDS7000. http://hds.leica-geosystems.com/downloads123/hds/hds/HDS7000/brochures-datasheet/HDS7000_DAT_de.pdf. Last access: 25.11.2015.

Lichti, D. D.; Lampard, J. (2008): Reflectorless total station self-calibration. Survey Review, Vol. 40, pages 244-259.

Lichti, D. D. (2010): Terrestrial laser scanner self-calibration: Correlation sources and their mitigation. ISPRS Journal of Photogrammetry and Remote Sensing, Vol. 65, pages 93–102.

Neitzel, F. (2006a): Gemeinsame Bestimmung von Ziel-, Kippachsenfehler und Exzentrizität der Zielachse am Beispiel des Laserscanners Zoller + Fröhlich Imager 5003. In: Luhmann/Müller [Hrsg.], Photogrammetrie - Laserscanning - Optische 3D-Messtechnik, Beiträge der Oldenburger 3D-Tage 2006, Herbert Wichmann Verlag.

Neitzel, F. (2006b): Untersuchung des Achssystems und des Taumelfehlers terrestrischer Laserscanner mit tachymetrischem Messprinzip. In: Beiträge zum 72. DVW-Seminar am 9. und 10. November 2006 in Fulda, Band 51, Wißner-Verlag.

Pelzer, H. (1985): Grundlagen der mathematischen Statistik und Ausgleichungsrechnung. In: H. Pelzer (Ed.), Geodätische Netze in Landes- und Ingenieurvermessung II. Konrad Wittwer Verlag, Stuttgart.

Rüeger, J. M. (1990): Electronic distance measurement: an introduction. Third totally revised edition, Springer-Verlag, Berlin.

Schäfer, Th. (2011): Flächenhafte Deformationsmessungen an Betonoberflächen unter Berücksichtigung der Interaktion Laserstrahl/Objektoberfläche; In: Photogrammetrie - Laserscanning - Optische 3D-Messtechnik, Beiträge der Oldenburger 3D-Tage 2011.

Schwieger, V. (1999): Ein Elementarfehlermodell für GPS Überwachungsmessungen. Schriftenreihe der Fachrichtung Vermessungswesen der Universität Hannover, Vol. 231.

Schwieger, V. (2001): Zur Konstruktion synthetischer Kovarianzmatrizen. ZfV - Zeitschrift für Vermessungswesen, 3/2001, S. 143-149.

Stahlberg, C. (1997): Eine vektorielle Darstellung des Einflusses von Ziel- und Kippachsenfehler auf die Winkelmessung. ZfV - Zeitschrift für Vermessungswesen, 5/1997, S. 225-235.

Zámečniková, M.; Neuner, H. (2014): Der Einfluss des Auftreffwinkels auf die reflektorlose Distanzmessung. In: Beiträge zum 139. DVW-Seminar am 11. und 12. Dezember 2014 in Fulda, Band 78, Wißner-Verlag.